THE ASTROPHYSICAL JOURNAL, 417:438–449, 1993 November 10

THE ANALYSIS OF GRAVITATIONAL LENS SURVEYS. I. SELECTION FUNCTIONS AND AMBIGUOUS CANDIDATES

CHRISTOPHER S. KOCHANEK[1]
Harvard-Smithsonian Center for Astrophysics, 60 Garden Street, Cambridge, MA 02138
Received 1993 March 22; accepted 1993 May 17

ABSTRACT

Our analysis of the four optical surveys for gravitational lenses shows that only one more lens is expected among the unidentified image pairs found in the surveys. The best candidates and the estimated likelihood that they are lenses are 0011−012 at 36%, 2355−019 at 26%, DW 0400+258 at 18%, and 1318+111 at 10% and potentially 0205−379 at 69% because its companion is identified as a star only by its red color. The distributions of unidentified candidates from Crampton et al. (1992) and the ESO/Liège Survey in both separation from the quasar and magnitude are consistent with the expected distribution of Galactic stars. Stars are a important source of background contamination in lens surveys, and stellar companions to quasars become more common than lensed images at the *confusion limit* of approximately 2.5 (1.2) mag fainter than 17 (19) V mag quasars. Cross-comparisons of candidates in the four surveys show that point-spread function asymmetries are an unreliable means of identifying lens candidates for statistical purposes because they have a very high false positive rate. These candidates must be excluded from statistical analyses of lens surveys. We estimate the completeness of the surveys is near 80% for lenses produced by E and S0 galaxies and near 70% for spiral galaxies. We use the incidence of quasar-quasar pairs in the sample to estimate that the quasar-quasar correlation length is between $1\ h^{-1}(1+z)^{-1}$ Mpc $\lesssim r_0 \lesssim$ $18\ h^{-1}\ (1+z)^{-1}$ Mpc, consistent with other measurements of quasar clustering.

Subject headings: cosmology: observations — gravitational lensing — surveys

1. INTRODUCTION

There are four large surveys for gravitational lenses among bright, high-redshift quasars (Crampton, McClure, & Fletcher 1992; Yee, Fillipenko, & Tang 1993; Surdej et al. 1993, hereafter the ESO/Liège Survey; and Bahcall et al. 1992, and Maoz et al. 1992, 1993a, b, hereafter the Snapshot Survey). The release of not only the lenses found in the surveys but also the candidate lists allows us to begin examining the theoretical implications of these surveys for the incidence of gravitational lenses, the masses of galaxies, and cosmology. This is the first in a series of papers that examine the problem of interpreting lens surveys in the presence of selection effects, and ambiguous candidates. A previous paper (Kochanek 1991) examined the effect on lens statistics of the procedures used to find quasars.

The largest homogeneous gravitational lens survey is the Snapshot Survey with 502 objects and five known lenses (0957+561, PG 1115+080, 1413+117, 1208+101, and 0142−100). There are also three ground-based optical surveys by Crampton et al. (1992) with 100 objects, Yee et al. (1993) with 108 objects and one known lens (1413+117), and the ESO/Liège Survey with 188 objects and four known lenses (PG 1115+080, 1413+117, 0142−100, and 1208+101). All these surveys selected high-redshift, high-luminosity quasars, and as a result there is a considerable overlap between the samples. If we exclude the five lenses, there are 888 observations of 648 distinct quasars between the four surveys: 453 were observed by only one survey, 162 by two surveys, 22 by three surveys, and 11 by all four surveys. The Snapshot Survey examined 54 Crampton et al. (1992) objects, 52 Yee et al. (1993) objects, and 111 ESO/Liège Survey objects leaving 322 unduplicated objects. Crampton et al. (1992) examined 34 Yee et al. (1993) objects and 15 ESO/Liège Survey objects leaving 32 unduplicated objects. Yee et al. (1993) examined 28 ESO/Liège Survey objects leaving 35 unduplicated objects, and the ESO/Liège Survey has 64 unduplicated objects. This duplication between the surveys provides an important means of controlling for differences in candidate identification.

The theoretical goal in examining these surveys is to use the incidence of gravitational lenses in the sample to estimate the masses of galaxies and the cosmological model. Such analyses are critically dependent on the completeness and contamination of the surveys. If the surveys are massively incomplete because the selection effects of the survey lead to the loss of large numbers of lenses, then the number of lenses found underestimates the true incidence of lenses. If the surveys are heavily contaminated with objects masquerading as lenses then the apparent number of lenses found overestimates the true incidence of lenses. The key to a reliable statistical analysis is to tune the model of the selection effects to estimate and control both of these problems.

Selection effects are caused by limitations on dynamic range, limitations on resolution, and the presence of confusing sources such as stars. Since the distribution of lenses extends to small separations and large dynamic ranges, limited resolution and dynamic range inevitably mean that some gravitational lenses present in the sample cannot be found. We call the rejection of a real lens because of selection effects a false negative. In a fixed set of observations, the number of false negatives can be reduced and the completeness of the survey increased by adopting a less restrictive selection function. The inverse of the problem of false negatives is the problem of false positives—treating objects which are not gravitational lenses as if they were. False positives arise either from an overly optimistic selection function that treats noise peaks or system-

[1] Alfred P. Sloan Research Fellow.

atic errors as candidates, or from real confusing sources such as stars, galaxies, and binary quasars.

The statistical analysis of a survey must balance itself between the Scylla of incompleteness and the Charybdis of ambiguity by choosing a selection function that maximizes the completeness without introducing too much contamination. The two problems which make a careful balance necessary are that gravitational lenses are rare (about 1% of bright quasars) and that the costs of pursuing additional observations of candidates are high. Rarity means that small systematic effects can create a pool of candidates dominated by false positives, while the high follow-up costs make it hard to separate the real lenses from the false positives. In § 2 we develop a statistical model for lenses so that we can examine these problems. In § 3 we treat the problem of contamination or false positives, emphasizing the unreliability of PSF asymmetries as a means of identifying lenses, and developing a statistical test for differentiating lenses from companion stars and quasars. In § 4 we examine the implications of the selection effects needed to avoid contamination on the completeness of surveys. In § 5 we review our conclusions and set the stage for the second paper in this series.

2. A STATISTICAL MODEL OF GRAVITATIONAL LENSES

Selection effects must be evaluated within the context of a specific statistical model. For the purposes of this paper we do not need a highly elaborate statistical model of gravitational lenses, but only a reasonable one. This allows us to model galaxy potentials as singular isothermal spheres, to use a Tully-Fisher (1977)/Faber-Jackson (1976) relation to connect rotation velocities or velocity dispersions to luminosities, and to model the distribution of galaxies in luminosity with a Schechter (1976) function. This is modeled on the analysis of Fukugita & Turner (1991).

A gravitational lens formed by a singular isothermal sphere of velocity dispersion σ produces two images separated by $\Delta\theta = 2b$, where $b = 4\pi(\sigma/c)^2 D_{\rm LS}/D_{\rm OS}$ is the critical radius of the lens, $D_{\rm LS}$ is the proper motion distance between the lens and source redshifts, and $D_{\rm OS}$ is the proper motion distance from the observer to the source (Gott & Gunn 1974). We use a constant comoving density of galaxies, a Tully-Fisher (1977)/Faber-Jackson (1976) type relation $L/L_* = (\sigma/\sigma_*)^4$, and a Schechter (1976) distribution of galaxies

$$\frac{dn}{dL} = \frac{n_*}{L_*}\left(\frac{L}{L_*}\right)^{-1} \exp\left(-L/L_*\right). \tag{2.1}$$

When we examine the absolute number of lenses, we treat only E and S0 galaxies for which $n_* = 0.005\ h^3\ {\rm Mpc}^{-3}$ using the estimates of galaxy number density from Efstathiou, Ellis, & Peterson (1988) and the relative numbers of S, S0, and E galaxies from Postman & Geller (1984), although we also address the completeness of the surveys for lenses produced by spiral galaxies. We use an Einstein–de Sitter cosmological model in which the matter density is equal to the critical density ($\Omega_M = 1$) and there is no cosmological constant, although the statistical results that do not depend on the absolute incidence of lenses are valid for all flat cosmologies.

With these assumptions, the optical depth for multiply imaging a quasar in a flat cosmology is

$$\tau = \frac{1}{30}\,\tau_*\, D_{\rm OS}^3\,, \tag{2.2}$$

where

$$\tau_* = 16\pi^3 n_*\, r_H^3 (\sigma_*/c)^4 = 0.032\left(\frac{\sigma_*}{250\ {\rm km\ s^{-1}}}\right)^4$$

$r_H = c/H_0$ is the Hubble radius, and $D_{\rm OS}$ is the proper motion distance to the quasar (Turner, Ostriker, & Gott 1984; Gott, Park, & Lee 1990; Turner 1990). The distribution of image separations $\theta = 2b$ in a flat cosmology is

$$\frac{1}{\tau}\frac{d\tau}{d\theta} = \frac{15}{b_*}\left(\frac{\theta}{2b_*}\right)^2\left\{\Gamma\left[-\frac{1}{2},\left(\frac{\theta}{2b_*}\right)^2\right] - \frac{\theta}{b_*}\,\Gamma\left[-1,\left(\frac{\theta}{2b_*}\right)^2\right] + \left(\frac{\theta}{2b_*}\right)^2\Gamma\left[-\frac{3}{2},\left(\frac{\theta}{2b_*}\right)^2\right]\right\}, \tag{2.3}$$

where $b_* = 4\pi(\sigma_*/c)^2 = 1\farcs8(\sigma_*/250\ {\rm km\ s^{-1}})^2$ is the critical radius scale for an L_* galaxy, and $\Gamma[a, b]$ is an incomplete gamma function (Kaiser & Tribble 1991; Fukugita & Turner 1991; Kochanek 1993). The mean image separation is $\langle\theta\rangle = b_*\,\Gamma[3/2] = 1\farcs6(\sigma_*/250\ {\rm km\ s^{-1}})^2$.

The differential probability distribution of magnifications produced by an SIS lens is

$$\frac{dP}{dM} = \frac{8}{M^3} \quad M > M_0 = 2 \tag{2.4}$$

and the flux ratio of the two images $f > 1$ is related to the total magnification by

$$M = 2\frac{f+1}{f-1} \tag{2.5}$$

(Gott & Gunn 1974). The number of lenses found in a real survey also depends on the magnitude distribution of the sources because of magnification bias (Gott & Gunn 1974; Turner 1980). We model the differential quasar distribution in magnitude as a broken power law

$$\frac{dN_q}{dm} = N_0\begin{cases}10^{\alpha(m-m_0)} & m < m_0\\ 10^{\beta(m-m_0)} & m > m_0\,,\end{cases} \tag{2.6}$$

where $N_0 = 10\ {\rm deg}^{-2}$, $m_0 = 19.15\ B$ mag, $\alpha = 0.86$, and $\beta = 0.28$ based on models of quasar distribution in the redshift range $0.5 \lesssim z \lesssim 2.5$ (Hartwick & Schade 1990). The two functions that we need to estimate the selection effects are the distribution of lenses in image separation and magnitude, and the distribution of the lenses in image separation and image magnitude difference. The probability that a quasar of magnitude m at proper motion distance $D_{\rm OS}$ is a lens with image separation θ and magnification M is

$$\frac{dP}{d\theta\,dM} = \frac{d\tau}{d\theta}\frac{dP}{dM}\frac{(dN_q/dm)(m + 2.5\log M)}{(dN_q/dm)(m)} = \frac{d\tau}{d\theta}\frac{8}{M^3}\frac{(dN_q/dm)(m + 2.5\log M)}{(dN_q/dm)(m)} \tag{2.7}$$

in the SIS model. If we define the magnitude difference between the two images to be $\Delta m = 2.5\log f$, where f is the flux ratio, then the probability distribution in image separation and magnitude difference is

$$\frac{dP}{d\theta\,d\Delta m} = 1.6\ln 10\,\frac{d\tau}{d\theta}\frac{f(f-1)}{(f+1)^3}\frac{(dN_q/dm)(m + 2.5\log M)}{(dN_q/dm)(m)}\,, \tag{2.8}$$

where the total magnitude of the images is m, the brighter image has magnitude $m + 2.5 \log (1 + f^{-1})$, and the fainter image has magnitude $m + 2.5 \log (1 + f)$, where $f \geq 1$.

3. CHARYBDIS: THE PROBLEM OF FALSE POSITIVES

There are two key points to keep in mind about controlling false positives. The first is that if the survey makes one mistake per 100 quasars in selecting candidates, most of the candidates will be false positives. The second is that the selection function used for doing statistical models of a survey can be (and should be!) more conservative than the detection limits of the survey. A conservative selection function has less sensitivity per quasar because it lowers the survey completeness, but it can improve the overall statistical model if it eliminates many ambiguous candidates. There are four primary sources of false positives: overly optimistic selection functions, randomly superposed stars, randomly superposed galaxies, and quasar companions.

Optimistic selection functions mainly play a role at small image separations because at large separations stars are the dominant problem rather than overestimates of dynamic range. The simplest check of the reliability of the selection functions at small separations is to compare small separation candidates between the various surveys. There are 12 candidates that lie outside the stated detection limits for the surveys, all but two of which are close, unresolved pairs (see Table 1). Seven of these 10 were examined and rejected by another survey, and in most of these cases it is a PSF subtraction residual from an optical survey being rejected by the more sensitive Snapshot Survey. Crampton et al. (1992) do not treat their three objects with PSF residuals as true lens candidates, and the Yee et al. (1993) examination of the three found either no residuals or unrepeatable residuals. There are two large separation and large dynamic range pairs that are detected by the ground-based surveys and not by the Snapshot Survey—although the candidates lie somewhat beyond the ground-based limits they are several magnitudes beyond the Snapshot limits. It is clear that PSF asymmetries are not a reliable means of recognizing candidates for statistical purposes, particularly when there is insufficient information to give a plausible measurement of the image separation and flux ratio. This means that the statistical properties of ground-based surveys should be evaluated using a more conservative selection function at small separations. It is empirically observed that the ESO/Liège Survey is much more optimistic in selecting candidates than the other three surveys.

Galactic stars are the primary source of real secondary images. We will use the analytic model from Bahcall & Soneira (1980) for the differential number counts of stars per square degree in the V band at magnitude m and Galactic coordinates l and b,

$$\frac{dN_*}{dm} = \frac{C_1 10^{\beta(m-m^*)}}{(1 + 10^{\alpha(m-m^*)})^{\delta}} \frac{1}{(\sin b - \mu \cos b \cos l)^{3-5\gamma}} + \frac{C_2 10^{\eta(m-m^\dagger)}}{(1 + 10^{\kappa(m-m^\dagger)})^{\lambda}} \frac{1}{(1 - \cos b \cos l)^{\sigma}}, \quad (3.1)$$

where $C_1 = 200$, $C_2 = 400$, $\alpha = -0.2$, $\kappa = -0.26$, $\beta = 0.01$, $\eta = 0.065$, $\delta = 2$, $\lambda = 1.5$, $m^* = 15$, $m^\dagger = 17.5$, $\mu = 0.03$ ($m < 12$), $0.0075\,(m - 12) + 0.03$ ($12 < m < 20$), 0.09 ($m > 20$), $\gamma = 0.36$ ($m < 12$), $0.04\,(12 - m) + 0.36$ ($12 < m < 20$), 0.04 ($m > 20$), and $\sigma = 1.45 - 0.20 \cos b \cos l$. Figure 1 compares the probability of finding a lensed image near a quasar as a function of magnitude to the probability of finding a star of the same magnitude within 3.″0 of the quasar. In this comparison we use a velocity dispersion scale of $\sigma_* = 270$ km s^{-1}, place the quasar at redshift $z_s = 2$, and use the stellar density normal to the Galactic plane ($l = 0°$, $b = 90°$).

Figure 1 also includes the distributions of galaxies, unrelated quasars along the line of sight, and correlated quasars. The

TABLE 1

AMBIGUOUS CANDIDATES

NAMES	z_s[a]	m_V[b]	$\Delta\theta$[c]	Δm[d]	SURVEYS[e] C	E	S	Y	COMMENTS AND NOTES
0013−004, UM 224	2.09	17.0	3.″2	5.6	y	y	n	y	Red color
0030+34, UM 45	1.90	18.4				y			
0033+098, 4C 09.1	1.92	17.5				y	N	n	
0100+130, PHL 957	2.68	16.6			y			n	
0438−166, 1E	1.96	17.7				y	N		
1017+280, TON 34	1.92	15.7		3.4				y	
1159+123	3.50	17.5	0.5	0.2		y	N		
1241+176	1.27	16.3	3.1	6.5		y	n		
1334−005, UM 590	2.79	17.0	0.2	0.5		y			
1448−232	2.21	17.0				y	N		
1623+268, SW 77	2.52	16.0			y			n	
2134+004, PKS	1.94	16.8			y	n	N	n	

[a] Quasar redshift.
[b] Quasar V magnitude.
[c] Angular separation to stellar companion.
[d] Magnitude difference between companion and quasar.
[e] Surveys which examined the quasar: C = Crampton et al. 1992, E = ESO/Liège, S = Snapshot Survey, Y = Yee et al. 1993. A y indicates that the survey may have detected something but it is either a PSF asymmetry or outside the selection function. A n indicates that the survey failed to detect something, but that the object lay outside the selection function. A N indicates that the survey should have detected any real companion found by the other methods. A Y indicates that the survey may have detected something and it lies inside the selection function—by definition, there are no Ys in this table. Separations $\Delta\theta$ and magnitude differences Δm are not available for many of the ESO/Liège Survey candidates.

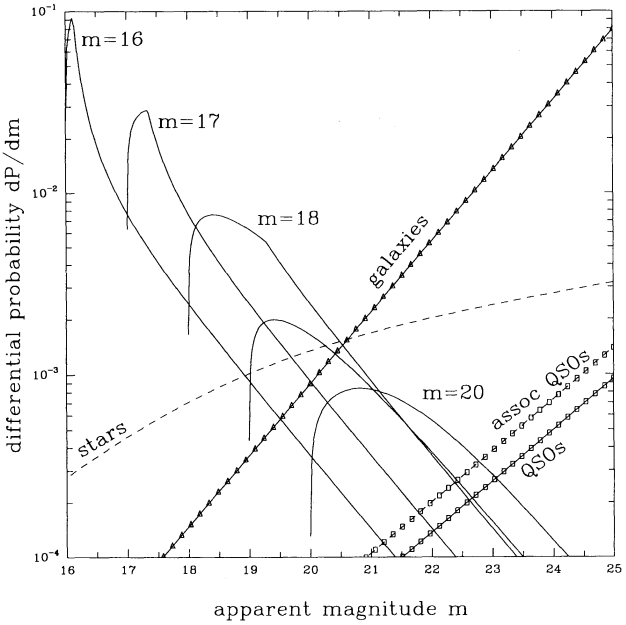

FIG. 1.—Probability distributions of quasar companions as a function of magnitude. The solid lines show the distribution in apparent magnitude of the fainter image for lenses with V magnitudes of 16, 17, 18, 19, 20 in an Einstein–de Sitter cosmology with a characteristic velocity dispersions for E and S0 galaxies of $\sigma_* = 270$ km s^{-1} for quasars at redshift $z_s = 2$. The dashed lines shows the distribution of stars in the direction normal to the Galactic plane within 3″ of the quasar. The solid line with triangles shows the estimated distribution of galaxies. The two solid lines with squares show the distribution of associated quasars from the two-point correlation function, and the distribution of unassociated quasars.

differential distribution of galaxies is $\log dN_g/dm = 0.39m - 5.19$ per square degree, based on the Tyson (1988) R counts combined with an average $V-R = 1$ mag color for galaxies at redshifts less than 1 (Coleman, Wu, & Weedman 1980). The density of unrelated quasars along the line of sight is given by the surface density of quasars (eg. [3.6]) used in computing the magnification bias. If we assume that quasars are clustered like galaxies with correlation function $\xi(r) = (r/r_0)^{-1.8}$ and $r_0 \simeq 5\ h^{-1}(1+z)^{-1}$ Mpc, and that the luminosities of clustered quasars are uncorrelated, then the surface density of clustered quasars in an Einstein–de Sitter universe is

$$\frac{dN_c}{d\theta\, dm} \simeq 10^{-7} \frac{dN_q}{dm} \left(\frac{\theta}{3''}\right)^{0.2} \times \left(\frac{r_0}{5\ h^{-1} x\ \mathrm{Mpc}}\right)^{1.8} \frac{x^{1.9}}{(x^{1/2}-1)^{0.9}}, \quad (3.3)$$

where $z = x - 1$ is the redshift of the quasar (Phinney & Blandford 1986).

The lensed images are strongly concentrated within a few magnitudes of the total magnitude of the lens, followed by a power-law tail at higher magnitudes [$\log (dN/d\Delta m) \propto -0.4\Delta m$]. For bright quasars ($m \lesssim 19$ B mag) the probability is completely dominated by the lens contribution in the region near the quasar. The next most important contribution comes from the slowly rising density of Galactic stars at fainter magnitudes. The rapid fall in the density of lensed images and the rising numbers of stars imposes a *confusion limit* on the observations when the density of stars becomes larger than the density of lensed companions. If we estimate the *confusion limit* as the magnitude difference at which the density of stars is equal to the density of lensed images we get $\Delta m \simeq 3$, 2.5, 2.5, and 1.2 mag for lens magnitudes of 16, 17, 18, and 19 V mag, respectively. For quasars with a V mag of 20, the density of stars is always larger than the density of lensed images. Reducing the quasar redshift from $z_s = 2$ to $z_s = 1$ lowers the density of lensed images by a factor of 3, and raising the redshift to $z_s = 4$ increases the density by a factor of 2. Most quasars are in fields with higher stellar densities than the direction normal to the plane (an average over a random sample of 50 survey QSOs gave an average increase in the stellar density at $m = 22$ of 2.3 times the density normal to the plane), so the density of stars in Figure 1 is a lower limit on the contamination. Thus the confusion limit always lies at much smaller magnitude differences than the theoretical detection limit of a ground-based survey—if you find a point source 5 mag fainter than a 16 mag quasar, the odds are 10:1 that it is a star even in fields with low stellar density.

For most of the quasar magnitudes examined in the bright surveys, stars are a greater problem than galaxies, and the galaxy confusion limit is larger than the stellar confusion limit. Moreover, star/galaxy separation can be effective even in a single image as long as the source is not near the detection threshold of the observation simply on the basis of morphology. If the selection function extends into the range where star/galaxy separation begins to break down, then the contamination from galaxies immediately dominates the sample. In this discussion we assume that the selection function is conservative enough to avoid confusing galaxies with point images.

Quasar companions are a negligible problem unless the dynamic range is very large. Even so, there is a confusion limit for quasars near $\Delta m = 5$, 5, 4.5, 3.5, and 2.5 mag for lenses with total magnitudes of 16, 17, 18, 19, and 20, respectively, with the contribution from associated quasars dominating that of the unassociated quasars at small separations ($\theta \lesssim 3''$). While this makes it a small effect, it is clearly detectable since the surveys contain at least one confirmed binary quasar (PHL 1222, Meylan et al. 1990, included in Yee et al. 1993 and the Snapshot Survey) and a second binary quasar/lens candidate 1120+019 = UM 425 (Meylan & Djorgovski 1989, included in the Snapshot Survey). Nonetheless, quasars are a negligible source of contamination for small separations and dynamic ranges where we expect to find most of the true lenses. If you look 4 mag fainter than a 18 mag quasar, the relative probabilities are 1:1:5 for finding a lensed image, a quasar, or a star, with the quasar being associated with the survey quasar about half the time.

Given the probability distributions in separation and magnitude, we can estimate the relative probabilities that an image found near a quasar is a lensed image, a star, or a different quasar. We assume that star/galaxy separation is possible, although there is no technical difficulty in adding a term for galaxies. The three probability densities for finding an image with magnitude $m + \Delta m$ distance θ from a quasar with magnitude m are equation (3.8) for lenses, $2\pi\theta(dN_*/dm)$ for stars, $2\pi\theta(dN_q/dm)$ for unassociated quasars, and equation (3.2) for associated quasars. In Table 2 we take each candidate pair from the four surveys and estimate the relative probabilities, using $\sigma_* = 270$ km s^{-1} and an Einstein–de Sitter cosmology for the lens model. This velocity dispersion is near the high end of the estimates for galaxies, but it is a little small for producing a lens like 0957+561.

TABLE 2

IMAGE PAIRS

Names (1)	z_s[a] (2)	m_V[b] (3)	$\Delta\theta$[c] (4)	Δm[d] (5)	Surveys[e] (6)	Lens[f] (7)	Star[g] (8)	QSO[h] (9)	Σ[i] (10)	Comments and Notes[j] (11)
1334−005, UM 590	2.79	17.0	0.″2	0.5	E	99%	1%		1.8	1
1208+101	3.80	18.1	0.5	1.5	E,S	94	5	0.7%	1.0	Lens
1715+535, PG	1.92	16.3	3.5	0.1	C,Y	90	10		1.9	Star
0205−379,	2.42	17.4	2.3	1.5	S	69	30	0.8	1.1	Red color
0142−100, UM 673	2.72	16.8	2.2	2.1	E,S,Y	67	32	1.3	0.7	Lens
0747+611	2.49	17.5	1.7	2.0	S	57	41	1.4	1.4	Star
1744+206	2.41	19.0	0.9	0.3	C	39	60	0.7	6.1	Star
0011−012	2.23	17.0	3.0	2.0	E	36	62	1.8	1.0	
2355−019	1.64	16.5	1.9	3.0	E	26	71	3.2	1.1	
0400+258, DW	2.11	18.0	3.2	0.7	C	18	82	0.2	5.3	
0957+561	1.41	16.8	6.2	0.3	S	17	83		0.8	Lens
0504+030, PKS	2.45	18.7	2.9	1.3	C,S	13	85	1.5	2.5	Star
1621+392	1.97	17.5	3.5	2.0	S	11	87	1.8	2.0	Star
1318+111	2.17	19.1	1.5	3.0	E	10	79	10	1.4	
2115−305, PKS	0.98	16.5	3.0	2.0	E	5	95	0.2	4.7	
1857+560, 4C 56.28	1.60	17.3	2.8	2.5	C,S	4	96	0.7	5.0	Red color
0202−512, JL 280	1.69	17.9	3.5	3.1	S	4	91	5.4	1.2	Cosmic ray?
1203−161, POX 61	2.46	17.8	2.3	4.2	S	4	88	7.5	1.8	Star
			6.1	0.0						Star
0007−427	2.67	18.3	2.4	4.5	E	3	85	12	1.6	
1766+237	1.72	18.0	4.6	0.7	S	3	97	0.1	7.4	Star
			4.1	4.0						Star
2021−330	1.47	19.5	1.8	1.5	S	2	97	0.9	9.4	2
0838+456, US 1498	1.41	17.6	4.4	3.4	S	0.9	93	5.8	1.0	
0552+39A, B 2	2.37	18.0	3.3	4.9	C	0.8	89	9.9	2.2	Galaxy(?)
0013−004, UM 224	2.09	17.0	3.2	5.6	C,E,S,Y	0.6	85	15	1.0	Red color
0420+003	2.92	19.1	4.4	3.4	E,S	0.6	89	11	1.3	3
1423+101	2.78	19.3	6.2	0.7	S	0.4	98	2.1	2.1	Red color
1120+019, UM 425	1.47	16.5	4.5	4.5	S	0.4	93	6.6	0.9	4
0151+048, PHL 1222	1.91	17.6	3.3	3.9	S,Y	0.3	87	9.7	0.8	Binary QSO
1311−270,	2.19	17.4	3.5	5.0	S	0.3	96	4.2	3.4	
2345+061, 4C 06.76	1.55	17.5	5.6	3.0	Y	0.3	96	4.1	1.1	Red color
0458−020, PKS	2.29	19.5	5.3	2.5	C,S	0.2	94	5.5	1.9	
1756+237, PKS	1.72	18.0	4.1	3.6	C,S	0.2	98	1.4	6.1	Star
2044−168	1.94	17.4	4.5	3.6	E	0.2	99	1.1	6.4	
1241+176	1.27	16.3	3.1	6.5	E,S	0.1	86	14	1.0	5
2118+168,	2.30	19.5	4.6	2.8	C		99	1.4	9.5	
0007+171, 4C 17.04	1.60	18.0	8.3	2.4	Y		97	3.4	1.2	Star
			10.5	4.0	Y					Star
0024+220	1.11	17.0	6.3	3.0	S		97	2.8	1.2	Similar color
0248+430	1.31	15.5	5.9	3.5	S		100	0.3	5.9	
0414+330	1.46	17.5	7.0	4.0	S		99	1.0	7.1	Red color
1237+134	1.73	17.8	6.9	3.2	S		95	5.3	1.1	
2000−330	3.78	19.0	4.9	3.6	E		99	1.3	13.3	
0034+024, UM 52	2.27	18.0	5.6	5.6	Y		81	19	0.9	Red color
0106+013, 4C 01.02	2.11	18.4	7.1	2.7	Y		93	7	0.8	
0119−046, 4C 04.04	1.95	16.9	8.0	5.2	Y		89	11	0.8	
0123+257, 4C 25.05	2.36	17.5	7.5	1.4	Y		99	0.9	1.6	Red color
0229+131, PKS	2.07	17.7	6.8	2.3	Y		96	3.8	0.9	Red color
1559+140	2.24	18.0	8.3	2.5	Y		99	1.2	3.9	
2333+019, PB 5468	1.87	18.0	6.8	3.0	Y		95	4.6	1.2	Red color
2203+290	4.41	20.7	6.0	0.0	C				5.3	Star
0812+332, B2	2.42	18.0	6.3	−0.9	Y				1.3	Brighter, red color
0941+261, B2	2.91	18.0	4.4	−0.3	S,Y				0.8	Brighter star
1315+665	1.98	18.9	5.6	−1.0	S				0.9	Brighter star

NOTE.—In cols. (7), (8), and (9), an empty entry indicates that the probability is less than 0.1%, except when the companion object is brighter than the quasar in which case the probabilities are not defined. When there are two companions, probabilities are given only for the brighter companion. All these systems are identified as stars.

[a] Quasar redshift.

[b] Quasar V magnitude.

[c] Angular separation to stellar companion.

[d] Magnitude difference between companion and quasar.

[e] Surveys that examined the quasar: C = Crampton et al. 1992, E = ESO/Liège, S = Snapshot Survey, Y = Yee et al. 1992.

[f] Probability in percent that the companion is a lens.

[g] Probability in percent that the companion is a star.

[h] Probability in percent that the companion is an (unlensed) quasar.

[i] Ratio of the stellar density at $m_V = 22$ in the direction toward the quasar to that in the direction normal to the Galactic plane ($b = 90°$).

[j] NOTES ON INDIVIDUAL OBJECTS.—(1). This companion is not detectable according to the ESO/Liège Survey selection function. See Table 1. (2). The quasar 2021−330 is listed in catalogs as being 16.5 mag and strongly variable. Maoz et al. 1992 show that the quasar is a nearby 19.5 mag object, and the strong variability comes from the 16.5 mag star's sometimes being called the quasar. (3). The Snapshot Survey found no companion for this quasar, although it should have been detectable with $\Delta\theta = 4.''4$ and $\Delta m = 3.4$. See Table 1. (4). This is a lens candidate as both images are quasars with nearly identical redshifts (Meylan & Djorgovski 1989). There is some evidence for a foreground cluster, so we may have underestimated the probability of it being a lens by treating only galaxies in determining the image separation distribution. (5). The Snapshot Survey found no companion, but with $\Delta m = 6.5$ it is much too faint. On the other hand it also lies outside the ESO/Liège selection function. See Table 1.

The three known two-image lenses in the surveys all have high probabilities of being lenses: 94% for 1208+101, 67% for 0142−100 = UM 673, and 17% for 0957+561. Even though the probability of large separations is suppressed by our mass model for the lenses, the lens 0957+561 still makes the list of the top 10 candidates despite its 6″.2 image separation. The ESO/Liège Survey candidate 1334−005 = UM 590 is probably a PSF subtraction artifact, and it certainly lies well past the limits of what the ESO/Liège Survey estimates can be detected. A *HST* snapshot would resolve the question, and it is probably worth checking because it is certainly a gravitational lens if it is real. If we treat 1334−005 = UM 590 as an artifact, then we expected to find 5.7 lenses among these candidates whereas we found only three. This is consistent with Poisson statistics. Moreover, we may have exaggerated the expected number of lenses by setting $\sigma_* = 270$ km s^{-1} near the upper limit of the expected range for galaxies, and we would obtain better agreement with the absolute number by using $\sigma_* = 220$ km s^{-1}.

There are four candidates from the ESO/Liège Survey and Crampton et al. (1992) that have at least a 10% probability of being lenses and have not been identified as stars: 0011−012 at 36%, 2355−019 at 26%, DW 0400+258 at 18%, and 1318+111 at 10%. The combined expectation that one of these objects is a lens is 90% which means that there is a 60% chance of finding that one of them is a lens under Poisson statistics. There is also one object (0205−379 at 69%) from the Snapshot Survey in which the companion is identified as a star based on its red color. While it is probable that it is a star, it is worth making sure with a spectrum since we know that there is differential reddening between the images of some of the known lenses that might also explain a redder color (e.g., Yee 1988 for 2237+0305). After these candidates there is a negligible chance for any of the remaining objects to be gravitational lenses—the aggregate probability for all the remaining unidentified candidates is less than 20%. Three of the surveys (Crampton et al. 1992, the Snapshot Survey, and Yee et al. 1993) have identified most of their candidates as stars, while it is unclear whether the ESO/Liège Survey has identified a population of stellar companions. It is important to perform these calculations using the actual Galactic coordinates of the survey quasar—if we computed the likelihood of DW 0400+258's being a lens using the stellar density at $(l, b) = (0°, 90°)$ instead of (162°,–14°) the probability of its being a lens rises to 80% because we have underestimated the surface density of stars by a factor of 6.

The expected number of quasar pairs in the sample is 1.6, almost evenly divided between unassociated (0.9) and associated (0.7), and the sample contains at least one associated quasar pair (0151+048 = PHL 1222) and probably a second (1120+019 = UM 425). The large flux ratio in the 1120+019 = UM 425 pair makes it highly unlikely that this object is a lens (15:1 against lensing) although the lens probability is also suppressed by the large separation (as in 0957+561). The upper limits on velocity differences in the wide quasar pairs are usually a few 100 km s^{-1}, which corresponds to a proper separation along the line of sight for UM 425 of $0.25\ h^{-1}(\Delta v/100\ \text{km s}^{-1})$ Mpc for pure Hubble flow, compared to the estimated correlation length $r_0 \simeq 2\ h^{-1}$ Mpc and a projected separation of only 20 h^{-1} kpc. At present we do not know how to weight the importance of these limits on the velocity difference between the two quasers in estimating the probability that this object is a lens. The presence of one or two associated quasars in this sample lets us estimate the correlation length of quasars, since the expected number scales as $0.7(r_0/5\ h^{-1}(1+z)^{-1}\ \text{Mpc})^{1.8}$. The best-fit correlation length to produce one associated quasar is $r_0 = 6\ h^{-1}(1+z)^{-1}$ Mpc, and the best fit to produce two associated quasars is $r_0 = 9\ h^{-1}(1+z)^{-1}$ Mpc. With only two objects, the limits on the possible range for r_0 are broad. If we define the range by the expectation values for which the probability of finding the observed number is only 10% of the peak probability, then the ranges for the correlation scale are $1\ h^{-1}$ Mpc $\lesssim r_0(1+z)^{-1} \lesssim 15\ h^{-1}$ Mpc or $3\ h^{-1}$ Mpc $\lesssim r_0(1+z)^{-1} \lesssim 19\ h^{-1}$ Mpc depending on the interpretation of 1120+019 = UM 425 as a lens or as an association. In either case, the range overlaps the correlation length found from studies of nearby galaxies extrapolated to the quasar redshifts (e.g., Shanks et al. 1987).

All these estimates are based only on the relative probabilities of an observed companion's being a lens, a star, or a quasar; we have not taken into account the actual numbers of objects that were observed. The reasoning is justified by the identification of the Yee et al. (1993) and the Snapshot Survey candidates as stars. Proving that the majority of these candidates are stars does not actually require identifying the candidates individually. We know the distribution of stars, so we can predict the statistical distribution of quasar-star pairs and compare it to the distribution of the observed candidates. Almost all the stars lie outside the quasar PSF, so we can treat the selection function as simply an outer radial cutoff for the area searched around each quasar and a uniform magnitude limit for finding stars within that area.

The first step is to use the radial distribution of the stars and stellar candidates to directly estimate the size of the area being surveyed. The integral distribution should simply be $\propto \pi\theta^2$ with a negligible correction for the region near the quasar. We include all candidates that are fainter than the quasar, and only the brightest companion when there are two near the quasar. In each survey we then use the Kolmogorov-Smirnov (K-S) test to estimate the probability that the stars are distributed uniformly over a disk with outer cutoff r_c. In each survey there is a well-defined optimal cutoff radius for the survey candidates and the probability that the data agrees with such a model is very high (>60%). The K-S test estimates of the survey areas are 5″.2 for Crampton et al. (1992), 4″.6 for the ESO/Liège Survey, 9″.5 for Yee et al. (1993), and 6″.4 for the Snapshot Survey. The angular cutoffs are only stated explicitly for Yee et al. (1993) (10″), and the Snapshot Survey (7″). The ESO/Liège Survey survey probably used 5″, and Crampton et al. (1992) probably used 6″. The radial distributions of the stars in each survey are shown in Figure 2 along with the best K-S fit to the distribution and the distribution estimated from the surveys. The agreement of a uniform distribution with the true distribution shows that almost all of these objects are simply stars independent of identifying the individual objects. For further calculations we use survey cutoff radii of $r_c = 6''$ for Crampton et al. (1992), 5″ for the ESO/Liège Survey, 7″ for the Snapshot Survey, and 10″ for Yee et al. (1993).

Once we know the area surveyed near each quasar we can use the number counts of stars to predict the distribution of the stars and stellar candidates in magnitude near the quasars. This tests both the hypothesis that the objects are stars, and it provides a means of estimating the average magnitude limits of the survey from the distribution of objects the survey detected. Since we are interested in dynamic range relative to the quasar, we take the list of survey quasars and predict the distribution of stars in magnitude difference from the quasars. We again

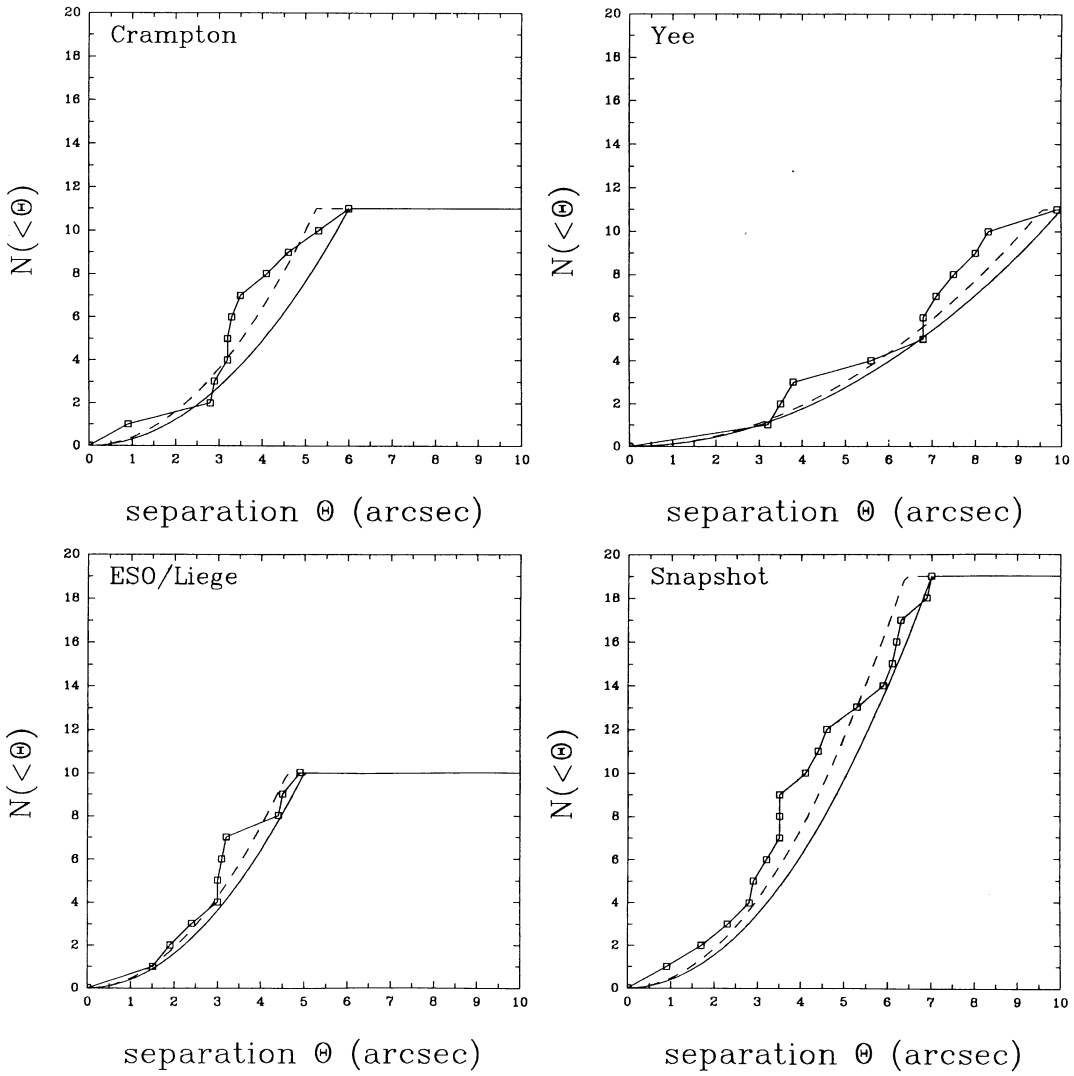

FIG. 2.—The integral distribution of stars and stellar candidates in distance from the quasar. The solid lines with squares show the observed distribution, the dashed line shows the best fit to the distribution, and the solid line shows either the reported or best guess for the survey cutoff.

include only the stars or stellar candidates fainter than the quasar, and only the brighter when there are two objects near the quasar. The predicted distributions for the four surveys are shown in Figure 3.

The candidates in the three ground-based surveys closely follow the predicted distribution of stars until $\Delta m \simeq 5$, which is also the estimated dynamic range of the three surveys. In the Snapshot Survey we must also include a detection limit of $m_V \simeq 21.5$ mag in the survey so the predicted number of stars flattens for differences greater than about 3 mag. Gould, Bahcall, & Maoz (1993) noted that the star counts in the Snapshot Survey fields also see fewer stars because the 279 Snapshot Survey quasars found in objective prism and other spectral surveys are selected to avoid quasars for which stars happened to lie inside the slit used for the survey. We also detect this effect in the region near the quasars as seen in Figure 3. If we crudely model this effect as 4″ wide zone of avoidance running across the quasar, then we will see roughly 80% of the stars predicted without the correction and this roughly brings the predicted and observed counts into agreement. This same effect modifies the star counts in the other three surveys, but there are too few objects to notice it.

Thus we can prove that the majority of the candidates are stars independently from the direct identifications by Yee et al. (1993) and the Snapshot Survey. These calculations confirm the estimates from the probability ratios in Table 2. Most of the unidentified companions in the ESO/Liège Survey are stars. Not only are they more likely to be stars than lenses based on their relative likelihoods, but they are also distributed in angle and magnitude like stars rather than lenses.

4. SCYLLA: THE PROBLEM OF FALSE NEGATIVES

The selection function is modeled by a limit on the magnitude difference between two images separated by angle θ, $\Delta m_L(\theta)$, which is equivalent to a limit on the flux ratio ($f > 1$) between the two images $\Delta m_L(\theta) = 2.5 \log f_L(\theta)$. The choice of this function is a combination of the physical detection limits of the device, the resolution of the particular observations, and our desire to avoid too many false positives. In the SIS model a

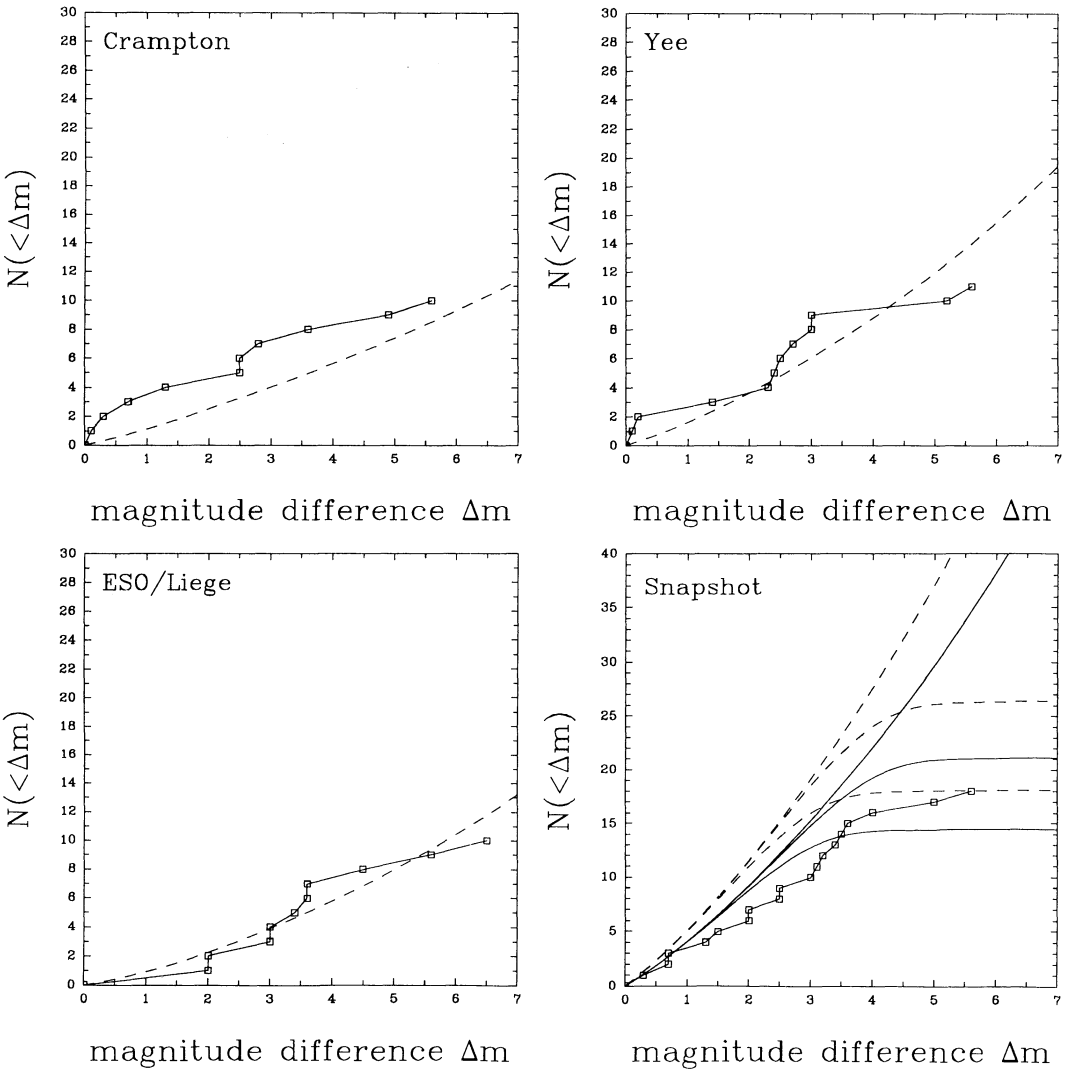

FIG. 3.—The integral distribution of stars and stellar candidates in magnitude difference from the quasar. The solid lines with squares show the observed distribution, and the dashed line shows the predicted distribution given the sample of observed quasars. In the snapshot survey the three dashed lines show no magnitude limit on the detection of stars, a limit of $m_V = 22$ mag, and a limit of $m_V = 21$ mag in order of predicting a smaller number of stars. The solid lines show the same curves after correcting expected number of stars near spectrally selected quasars as discussed in the text.

limit on the dynamic range sets a lower limit on the magnification of

$$M \geq M_L(\theta) = 2\left[\frac{f_L(\theta)+1}{f_L(\theta)-1}\right] \geq 2 \tag{4.1}$$

so that the probability of finding that a quasar of magnitude m and redshift z_S is a lens in the presence of the selection function is

$$p_L = \int_0^\infty d\theta \int_{M_L(\theta)}^\infty \frac{dP}{d\theta\, dM}\,. \tag{4.2}$$

compared to

$$p_0 = \int_0^\infty d\theta \int_2^\infty \frac{dP}{d\theta\, dM} \tag{4.3}$$

with no selection function. It is essential to formulate the selection effects including the modifications to the amount of magnification bias—simply modifying the optical depth (3.2) greatly overestimates the effects of limited dynamic range. This was done correctly in the Monte Carlo simulations of Kochanek (1991), and most other studies have avoided the question by using selection functions that find either all or none of the lenses of a given separation. This effect is critical because in a sample of bright quasars almost all the lenses are highly magnified, which means that the flux ratios are not very large (eq. [3.5]) and limits on dynamic range do not have a dramatic effect on the completeness of bright lens surveys ($m \lesssim 18$). The completeness of the survey is estimated by the ratio of the probability of finding lenses with the selection function to that without the selection function, p_L/p_0, and the fraction of false negatives is $1 - p_L/p_0$. In flat cosmologies using the SIS lens model, the completeness is independent of the quasar redshift and depends only on the quasar magnitude and the velocity dispersion scale σ_* (because it sets the separation scale for the lenses).

In the previous section we discussed what constraints must be placed on the selection function to control the problem of contamination. In particular, the surveys must use conservative estimates of the selection function at small separations to avoid the problems associated with ambiguous candidates produced by PSF asymmetries. Again, the reason is not that PSF analyses cannot detect some small separation lenses, but that they also produce false detections that contaminate the result. The magnitude counts of stars confirm that the detection limit of the ground-based optical surveys at large separations is about 5 mags as the surveys had estimated, while the Snapshot Survey limit is approximately 3–4 mag combined with an absolute cutoff at approximately $m_V = 21.5$ mag. Because of the ambiguities introduced by the image trails in the Snapshot Survey, we use an ultraconservative model for the magnitude difference limit of 3 mag. The selection function must also include the radial cutoffs r_c for the search area that we estimated in § 3.

The ambiguous small separation candidates in the ground-based surveys all lie outside the selection functions estimated by the surveys themselves. This suggests that the selection functions are reasonable estimates of the detection limits, but that they have not actually been used to select candidates. Thus for concrete models of the selection effects in the ground-based surveys we use some of the Surdej et al (1993) models for the selection effects in the four optical surveys with the important addition of the radial cutoff r_c. The first selection function models ground-based observations with only visual examinations for candidates in seeing with a full width at half-maximum of $\Delta\theta$:

$$\Delta m(\theta) = \begin{cases} \text{no solution} & \theta < 0.45\Delta\theta \\ -7.5 + 16.67\,\dfrac{\theta}{\Delta\theta} & 0.45\Delta\theta < \theta < 0.75\Delta\theta \\ 5 & 0.75\Delta\theta < \theta < r_c \end{cases} \tag{4.4}$$

the second selection function models ground-based observations with point-spread function subtraction on the candidates

$$\Delta m(\theta) = \begin{cases} \text{no solution} & \theta < 0.20\Delta\theta \\ -1.82 + 9.09\,\dfrac{\theta}{\Delta\theta} & 0.20\Delta\theta < \theta < 0.75\Delta\theta \\ 5 & 0.75\Delta\theta < \theta < r_c \end{cases} \tag{4.5}$$

and the third models the Snapshot Survey selection function

$$\Delta m(\theta) = \begin{cases} \text{no solution} & \theta < 0\farcs12 \\ 0.300 + 5.883\theta & 0\farcs12 < \theta < 0\farcs46 \\ 3 & 0\farcs46 < \theta < 7\farcs0\,. \end{cases} \tag{4.6}$$

These simple functions, which are shown in Figure 4, were chosen by Surdej et al. (1993) and they tend toward overestimating the capabilities of ground-based observations at small separations and underestimating the capabilities of the Snapshot Survey at large separations. The average seeing in the ground-based surveys is about FWHM = 1″.0 for ESO/Liège Survey, 0″.75 for Yee et al. (1993), and 0″.65 for Crampton et al. (1992).

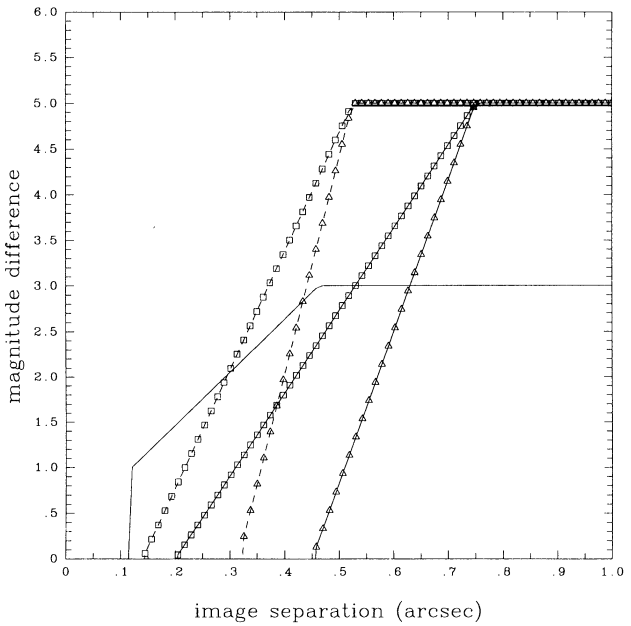

FIG. 4.—Survey estimates of selection functions defined by the flux ratio in magnitudes $\Delta m(\theta)$ which can be detected for images separated by angle θ. The solid line is the estimate for the Snapshot Survey, the lines with triangles are for ground-based observations without careful PSF subtraction, and the squares are for ground-based observations with careful PSF subtraction. The solid lines for the ground-based observations show the selection functions in 1″.0 FWHM seeing, and the dashed lines show the selection functions in 0″.7 FWHM seeing.

Given these definitions of the selection functions we compute the survey completeness both as a function of image separation,

$$c(\theta) = \left(\int_{M_L(\theta)}^{\infty} dM\,\frac{dP}{d\theta\,dM}\right)\left(\int_{2}^{\infty} dM\,\frac{dP}{d\theta\,dM}\right)^{-1}, \tag{4.7}$$

and velocity dispersion scale,

$$c(\sigma_*) = \frac{p_L}{p_0}\,. \tag{4.8}$$

Figure 5 shows the completeness as a function of image separation and lens magnitude for the four surveys, and Figure 6 shows the completeness for the surveys as a function of the mass scale σ_* of the galaxy distribution. In the ground-based surveys we include both estimates for the selection function at small image separations. High resolution strongly favors the Snapshot Survey at small separations and mass scales, but high dynamic range favors ground-based surveys for large separations and fainter lenses. The size of the survey region modifies the sensitivity of the survey to large separations and mass scales, and for the ESO/Liège Survey the outer survey radius begins to have an effect at the velocity dispersion scale for galaxies.

The completeness as a function of velocity dispersion scale is included because the appropriate values for σ_* are not accurately known. The typical velocity dispersion scale for spiral galaxies is small ($\sigma_* \simeq 150$ km s^{-1}), and ground-based surveys can find at most 45%–75% of the lenses produced by such a population at the mean magnitude of the quasars in the surveys ($\langle m\rangle \simeq 18$), while the Snapshot Survey could find about 75% of such lenses. In this limit the primary factor is the

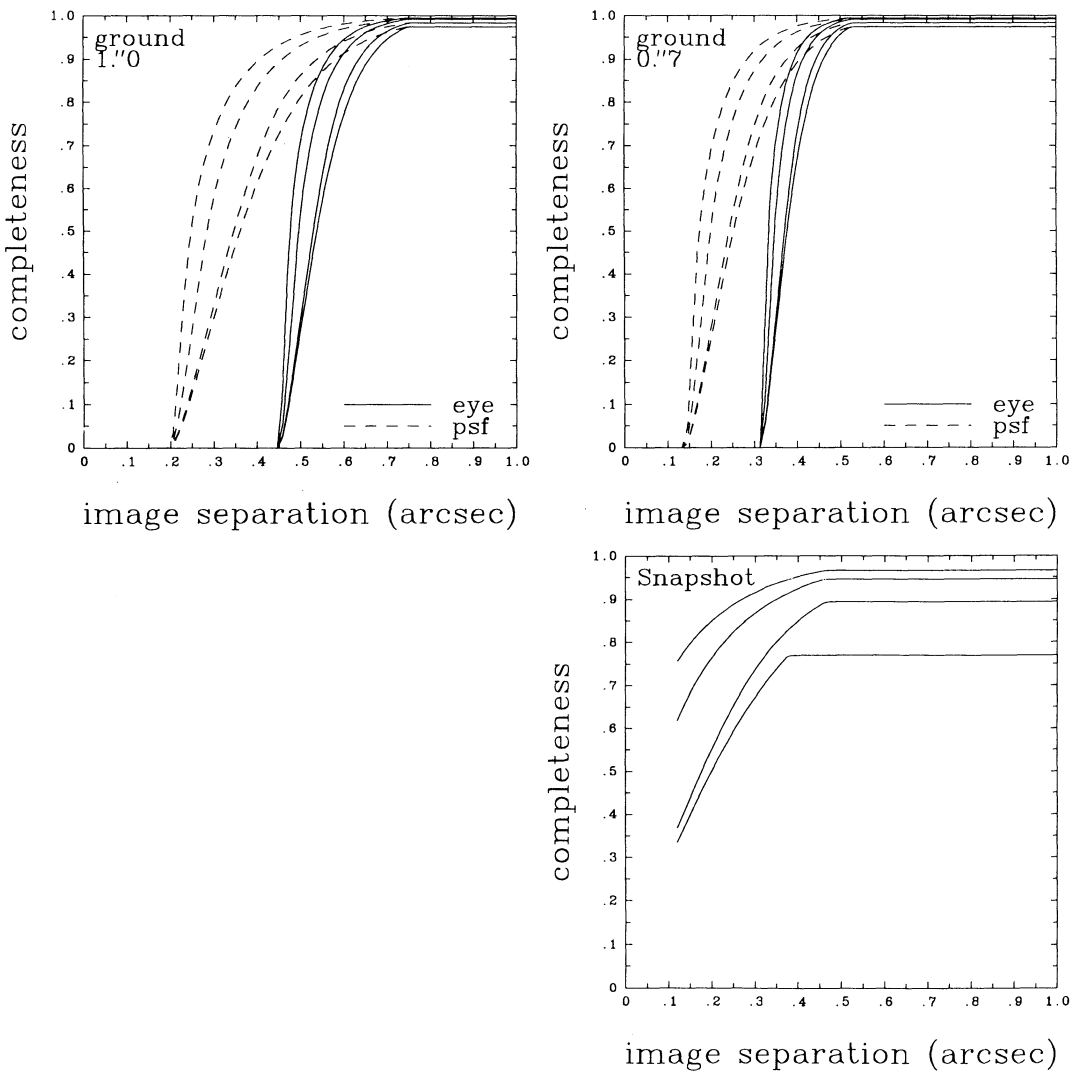

FIG. 5.—Estimates of survey completeness as a function of image separation. The ground-based estimates are shown for seeing FWHM of 1."0 and 0."7 and for the estimate of the "by eye" selection function from eq. (4.4) (*solid*), and the "PSF subtraction" selection function from eq. (4.5) (*dashed*). The completeness is shown for 16, 17, 18, and 19 mag lenses with the completeness decreasing as the quasar becomes fainter.

higher resolution of *HST*. Spirals are expected to produce only a small fraction of the total number of lenses, so that incompleteness in this range may not be important for overall completeness in the survey. The measured velocity dispersions of E and S0 galaxies are $\sigma_* \simeq 220$ km s^{-1}, and at this velocity dispersion the completeness is about 85% for the Snapshot Survey and 80%–90% for ground-based surveys. Theoretical arguments about dark matter in E and S0 galaxies suggest that the velocity dispersion of the mass distribution may be $(3/2)^{1/2}$ larger than that of the luminous material (Gott 1977; Turner et al. 1984). If $\sigma_* \simeq 270$ km s^{-1} the completeness is about 85% for the Snapshot Survey and 90–95% for Crampton et al. (1992) and Yee et al. (1993). The completeness of the ESO/Liège Survey is lower at 80%–85% because the small search region ($r_c \simeq 5''$) reduces its sensitivity to large separation lenses. For quasars brighter than 18 mag the balance shifts more in favor of the Snapshot Survey (at $\sigma_* = 220$ km s^{-1} and 17 mag the completeness is 86%–94% for ground-based and 92% for the Snapshot Survey), and for quasars fainter than 18 mag the balance shifts more in favor of ground-based surveys (at $\sigma_* = 220$ km s^{-1} and 19 mag the completeness is 76%–91% for ground-based and 81% for the Snapshot Survey).

In any case, the current surveys are good enough to detect most of the lenses expected from the predicted mass distributions of galaxies. Note that these estimates of the completeness are the same for all flat cosmologies, because the distribution of image separations (eq. [2.3]) is the same in all flat cosmologies, and the magnification bias is independent of cosmology in the SIS lens model. The combined surveys have found five gravitational lenses, and these estimates of the completeness suggests that the surveys miss only one lens on average due to problems of completeness arising from the selection function. This is considerably less than the variations expected from simple Poisson fluctuations in the number of lenses.

5. DISCUSSION

The consideration of completeness and contamination leads us to the following conclusions about the optical surveys for gravitational lenses.

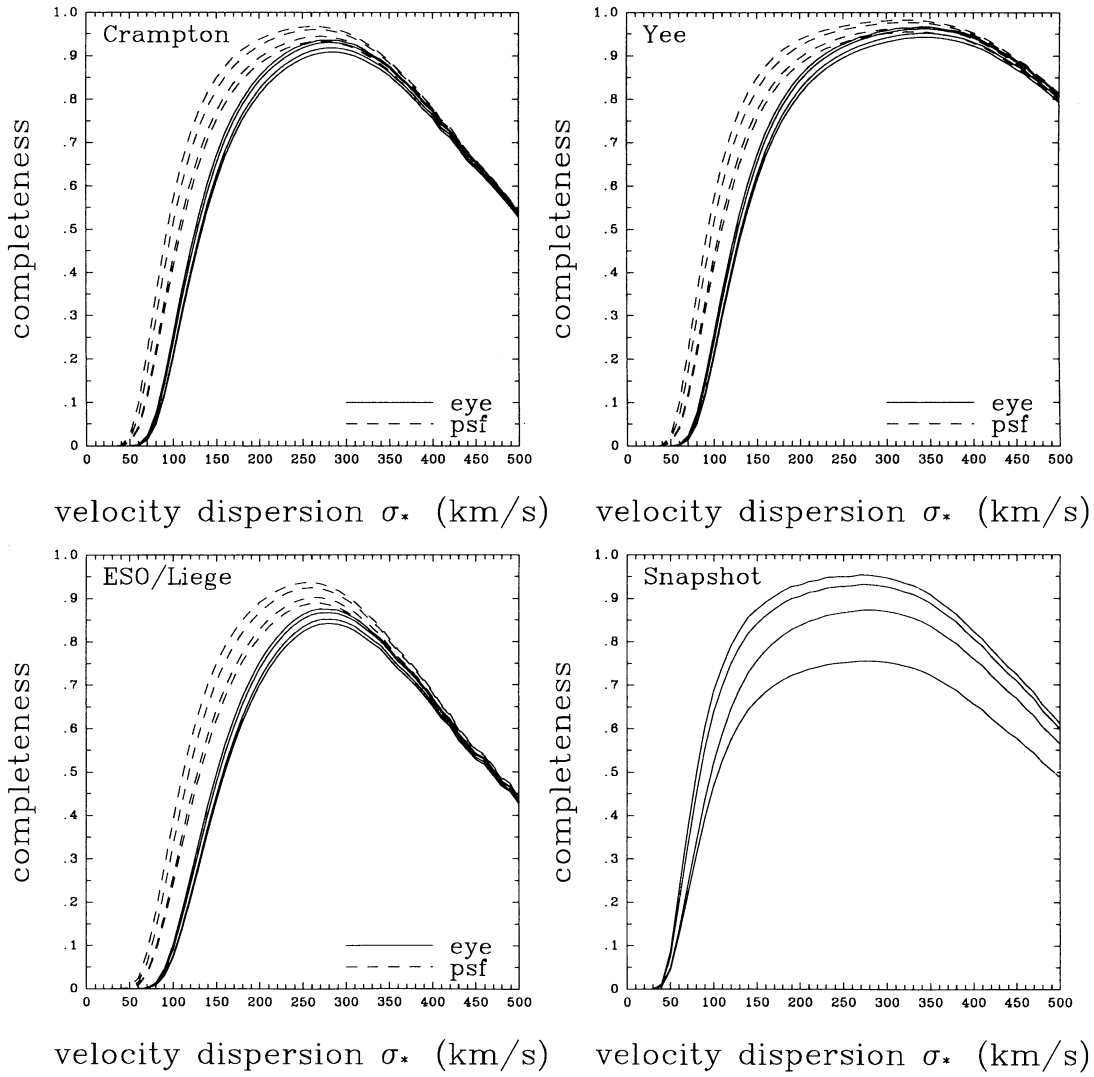

FIG. 6.—Estimates of survey completeness as a function of characteristic galaxy velocity dispersion σ_*. The completeness includes the estimate of the size of the area surveyed for lensed images which leads to a cutoff at large velocity dispersions. The seeing assumed for the ground-based surveys is 0.″7 for the Crampton et al. (1992) and Yee et al. (1993) surveys, and 1.″0 for the ESO/Liège Survey. These are near the average values for the three surveys. The selection function is shown for 16, 17, 18, and 19 mag lenses with the completeness decreasing as the quasar becomes fainter. Both the "by eye" (eq. [4.4], *solid*) and "PSF subtraction" (eq. [4.5], *dashed*) selection functions are shown for the ground-based surveys.

1. The ground-based surveys have not treated their "selection functions" as a real selection functions, because they frequently include candidates that are outside their limits. Selection functions must be specified and used in the statistical analysis if the results are to have any meaning. We can fix this in statistical analyses by eliminating the candidates that do not meet this criterion.

2. At small separations, PSF subtraction is demonstrably unreliable as a means of identifying candidates for statistical purposes. While it will sometimes identify real lenses (e.g., 1208+101 in the ESO/Liège Survey), it finds a much larger number of dubious candidates as demonstrated by comparing the small separation pairs and PSF asymmetries found in the various surveys. These objects should be pursued to see if they are lenses, but we cannot use them for statistical studies until a reliable means of eliminating the false positives is found. Yee et al. (1993), Crampton et al. (1992), and the Snapshot Survey were conservative in interpreting these candidates, while the ESO/Liège Survey appears to be too liberal.

3. A large dynamic range in the selection function increases the fraction of lenses that can be found, but it also dramatically increases the number of false positives if it exceeds the confusion of approximately 3 mag fainter than the quasar. Higher dynamic range adds only a small number of additional lenses (about 10% of the total for the typical survey magnitude of 18) but a huge number of random quasar-star, quasar-galaxy, and quasar-quasar pairs. In statistical studies it is better to reduce the survey completeness by adopting a restricted dynamic range because it eliminates most of the ambiguous candidates.

4. Selection functions are also truncated at an outer separation scale. This scale is not always specified, and it varies from survey to survey, In Yee et al. (1993) it is 10″, and in the Snapshot Survey it is 7″. In Crampton et al. (1992) we estimate that it is 6″, and in the ESO/Liège Survey we estimate that it is

5″ based on the distribution of stars in the sample. The location of this cutoff can have a significant impact on the completeness of the survey.

The most significant source of contamination in the surveys comes from randomly associated stars near the quasar. The known number counts of stars can be combined with a model for lens statistics to estimate the likelihood that any image pair is a lens or simply a star. Most of the candidate image pairs are predicted to be quasar-star pairs. This is confirmed by both the direct identification of many of the Yee et al. (1993), Crampton et al. (1993), and Snapshot Survey candidates as stars, and a statistical analysis of the candidates to show that they have the same spatial and flux distributions as stars. To evaluate the list of lens candidates found by a survey, we need to know the number and distribution of stars found by the survey. We can predict the expected number of stars found by a survey accurately, and this background signal must be accounted for by the surveys.

The known lenses in these samples all have significant probabilities of being lenses under our statistical test, ranging from 94% for 1208+101 down to 17% for 0957+561. The mass model used for the lens statistics may lead to an underestimate of the likelihood that 0957+561 is a lens because of the large separation between the images. Only four of the remaining Crampton et al. (1993) and ESO/Liège Survey candidates have a greater than 10% chance of being a gravitational lens: 0011−012 at 36%, 2355−019 at 26%, 0400+258 at 18%, and 1318+111 at 10%. The Snapshot Survey candidate 0205−379 is identified as a star based on colors, but a more careful identification should be considered because obscuration by a lens galaxy can also produce color differences. The combined expectation value suggests that we expect one additional lens among the remaining candidates, although we could easily find none because of Poisson statistics.

The estimated completeness of the optical surveys for lenses produced by elliptical galaxies is 80%–90%. This implies that less than one lens is missed for each five that are found. The completeness for lenses produced by spiral galaxies is much lower in the ground-based surveys particularly if a conservative approach is taken on PSF subtraction, but it is still near 75% for the Snapshot Survey. In practice the completeness is probably somewhat higher because the model of the selection function used for the Snapshot Survey may be too conservative, and because a large part of the sample was observed by both ground-based surveys and the Snapshot Survey. This part of the sample benefits from both the high resolution of the Snapshot Survey, and the high dynamic range of the ground-based surveys. A full statistical analysis of the surveys should use the superposition of the selection functions for each of the surveys that examined the quasar.

It is very unlikely that the quasar pair 1120+019 = UM 425 is in fact a gravitational lens. Both the image separation and the magnitude difference are much larger than expected for a gravitational lens. It is 6 times more likely to be an associated quasar pair if we assume that quasars are clustered like galaxies. There also is one real quasar pair, 0151+048 = PHL 1222, in the sample, and we can use the likelihood of finding these objects to estimate the correlation length at these redshifts. If we use the standard scaling for the correlation length, $r_0 \propto (1+z)^{-1}$, we estimate that the quasar-quasar correlation length is $r_0 = 6\ h^{-1}(1+z)^{-1}$ to $9\ h^{-1}(1+z)^{-1}$ Mpc depending on whether we include 1120+019 = UM 425 as a lens or a quasar pair. The probability of the fit to r_0 drops to 10% of the value of the peak at the edges of the range $1\ h^{-1}(1+z)^{-1}$ Mpc $\lesssim r_0 \lesssim 18\ h^{-1}(1+z)^{-1}$ Mpc. This is consistent with other studies of the quasar correlation function (e.g., Shanks et al. 1987).

This research was supported by a fellowship from the Sloan Foundation.

REFERENCES

Bahcall, J. N., & Soneira, R. M. 1980, ApJS, 44, 73
Bahcall, J. N., Maoz, D., Doxsey, R., Schneider, D. P., Bahcall, N. A., Lahav, O., & Yanny, B. 1992, ApJ, 387, 56
Coleman, G. D., Wu, C.-C., & Weedman, D. W. 1980, ApJS, 43, 393
Crampton, D., McClure, R. D., & Fletcher, J. M. 1992, ApJ, 392, 23
Efstathiou, G., Ellis, R. S., & Peterson, B. A. 1988 MNRAS, 232, 431
Faber, S. M., & Jackson, R. E. 1976, ApJ, 204, 668
Fukugita, M., & Turner, E. L. 1991, MNRAS, 253, 99
Gott, J. R. 1977, ARA&A, 15, 235
Gott, J. R., & Gunn, J. E. 1974, ApJ, 190, L105
Gott, J. R., Park, M.-G., & Lee, H. M. 1989, ApJ, 338, 1
Gould, A., Bahcall, J. N., & Maoz, D. 1993, ApJS, 88, 53
Hartwick, F. D. A., & Schade, D. 1990, ARA&A, 28, 437
Kaiser, N., & Tribble, P. 1991, in The Space Distribution of Quasars, ed. D. Crampton (ASP Conf. Series 21), 304
Kochanek, C. S. 1991, ApJ, 379, 517
———. 1993, MNRAS, 261, 453
Maoz, D., Bahcall, J. N., Doxsey, R., Schneider, D. P., Bahcall, N. A., Lahav, O., & Yanny, B. 1993a, ApJ, 402, 69
Maoz, D., et al. 1993b, ApJ, in press
Maoz, D., Bahcall, J. N., Schneider, D. P., Doxsey, R., Bahcall, N. A., Lahav, O., & Yanny, B. 1992, ApJ, 394, 51
Meylan, G., & Djorgovski, S. 1989, ApJ, 338, L1
Meylan, G., Djorgovski, S., Weir, N., & Shaver, P. 1990, in Lecture Notes in Physics 360, Gravitational Lensing, ed. Y. Mellier et al. (Berlin: Springer-Verlag), 111
Phinney, E. S., & Blandford, R. D. 1986, Nature, 321, 569
Postman, M., & Geller, M. J. 1984, ApJ, 281, 95
Schechter, P. 1976, ApJ, 203, 297
Shanks, T., Fong, R., Boyle, B. J., & Peterson, B. A. 1987, MNRAS, 227, 739
Surdej, J., et al. 1993, AJ, 105, 2064 (ESO/Liège Survey)
Tully, R. B., & Fisher, J. R. 1977, A&A, 54, 661
Turner, E. L. 1980, ApJ, 242, L135
———. 1990, ApJ, 365, L43
Turner, E. L., Ostriker, J. P., & Gott, J. R. 1984, ApJ, 284, 1
Tyson, J. A. 1988, AJ, 96, 1
Yee, H. K. C. 1988, AJ, 95, 1331
Yee, H. K. C., Fillipenko, A. V., & Tang, D. 1993, AJ, 105, 7